Biogeosciences Discuss., https://doi.org/10.5194/bg-2019-180
Manuscript under review for journal Biogeosciences
Discussion started: 23 May 2019

Biogeosciences Discussions Open Access EGU

The pH dependency of the boron isotopic composition of diatom opal (*Thalassiosira weissflogii*)

Hannah K. Donald[1], Gavin L. Foster[1,*], Nico Fröhberg[1], George E. A. Swann[2], Alex J. Poulton[3,4], C. Mark Moore[1] and Matthew P. Humphreys[1,5]

[1]School of Ocean and Earth Science, National Oceanography Centre Southampton, University of Southampton, Southampton, SO14 3ZH
[2]School of Geography, University of Nottingham, University Park, Nottingham, NG7 2RD
[3]Ocean Biogeochemistry and Ecosystems, National Oceanography Centre, Southampton, SO14 3ZH
[4]The Lyell Centre, , Heriot-Watt University, Edinburgh, EH14 4AS
[5]School of Environmental Sciences, University of East Anglia, Norwich, NR4 7TJ
*Corresponding Author

Abstract

The high latitude oceans are key areas of carbon and heat exchange between the atmosphere and the ocean. As such, they are a focus of both modern oceanographic and palaeoclimate research. However, most palaeoclimate proxies that could provide a long-term perspective are based on calcareous organisms, such as foraminifera, that are scarce or entirely absent in deep-sea sediments south of 50° latitude in the Southern Ocean and north of 40° in the North Pacific. As a result, proxies need to be developed for the opal-based organisms (*e.g.* diatoms) that are found at these high latitudes, and which dominate the biogenic sediments that are recovered from these regions. Here we present a method for the analysis of the boron (B) content and isotopic composition ($\delta^{11}B$) of diatom opal. We also apply it for the first time to evaluate the relationship between seawater pH and $\delta^{11}B$ and B concentration ([B]) in the frustules of the diatom *Thalassiosira weissflogii,* cultured at a range of pCO_2/pH. In agreement with existing data, we find that the [B] of the cultured diatom frustules increases with increasing pH (Mejia et al., 2013). $\delta^{11}B$ shows a relatively well-defined negative trend with increasing pH; a completely distinct relationship from any other biomineral previously measured. This relationship not only has implications for the magnitude of the isotopic fractionation that occurs during boron incorporation into opal, but also allows us to explore the potential of the boron-based proxies for palaeo-pH and palaeo-CO_2 reconstruction in high latitude marine sediments that have, up until now, eluded study due to the lack of suitable carbonate material.

Biogeosciences Discuss., https://doi.org/10.5194/bg-2019-180
Manuscript under review for journal Biogeosciences
Discussion started: 23 May 2019

1. Introduction

The high latitude regions, such as the Southern Ocean and the subarctic North Pacific, exert key controls on atmospheric CO_2. Both areas are where upwelling of deep carbon- and nutrient-rich water occurs, which promotes outgassing of previously stored carbon to the atmosphere and nutrient fertilisation of primary productivity, in turn drawing down CO_2. The balance of processes involved in determining whether these oceanic regions are a source or sink of CO_2 are poorly understood, to the extent that the oceanic controls on glacial-interglacial pH and pCO_2 changes remain a subject of vigorous debate (*e.g.* Martin, 1990; Sigman and Boyle, 2000). Recently, several studies have shown how the boron isotope pH proxy applied to calcitic foraminifera successfully tracks surface water CO_2 content, and thus documents changes in air-sea CO_2 flux along the margins of these regions (*e.g.* Martínez-Botí et al., 2015; Gray et al. 2018). However, the lack of preserved marine carbonates in areas that are thought to be key in terms of glacial-interglacial CO_2 change (*e.g.* the polar Antarctic zone; Sigman et al., 2010) represents a currently insurmountable problem, and prevents the determination of air-sea CO_2 flux using boron-based proxies in regions that are likely to play the most important role in glacial-interglacial CO_2 change. There is therefore a clear need for the boron isotope palaeo-pH proxy to be developed in biogenic silica (diatom frustules, radiolarian shells), which is preserved in high-latitude settings, to better understand these key regions and their role in natural climate change.

The boron isotopic system has been used extensively in marine carbonates for the reconstruction of past ocean pH, and past atmospheric CO_2 (*e.g.* Hemming and Hanson, 1992; Pearson and Palmer, 2000; Hönisch and Hemming, 2005; Foster, 2008; Henehan et al., 2013; Chalk et al. 2017; Sosdian et al. 2018). Comprehensive calibration work has been completed for numerous species of foraminifera that are currently used in palaeoceanographic reconstruction (*e.g.* Henehan et al. 2016; Rae et al. 2011), and it has been shown that while $\delta^{11}B$ compositions are fairly similar among carbonates, species-specific differences exist in the relationship between the boron isotopic composition of dissolved borate and the $\delta^{11}B$ of foraminifera. Once this relationship is known, this $\delta^{11}B$-pH calibration can be applied to fossils found in deep-sea sediment cores, reliably reconstructing past ocean pH and pCO_2 (*e.g.* Hönisch and Hemming, 2005; Foster, 2008, Hönisch et al., 2009; Chalk et al., 2017). However, thus far the boron isotopic composition (expressed as $\delta^{11}B$) and B concentration ([B]) of the siliceous fraction of deep sea sediments remains poorly studied.

Early exploratory work by Ishikawa and Nakamura (1993) showed that biogenic silica and diatom ooze collected from modern deep sea sediments in the North and Equatorial Pacific had relatively high

Biogeosciences Discuss., https://doi.org/10.5194/bg-2019-180
Manuscript under review for journal Biogeosciences
Discussion started: 23 May 2019

boron contents (70-80 ppm), but a very light isotope ratio. For example, a diatom ooze was shown to have a $\delta^{11}B$ of -1.1 ‰ whilst radiolarian shells had a $\delta^{11}B$ of +4.5 ‰. While some of this light $\delta^{11}B$ may have partly arisen due to clay contamination (reducing the diatom ooze sample by up to 3 ‰; Ishikawa and Nakamura, 1993) it also likely reflects an opal:seawater isotopic fractionation arising from the substitution of borate for silicate in tetrahedral sites in the opal (Ishikawa and Nakamura, 1993). A similarly light $\delta^{11}B$ was also observed in marine cherts from deep sea sediments by Kolodny and Chaussidon (2004; -9.3 to +8 ‰), but these are unlikely to be primary seawater precipitates. A recent culture study of the diatoms *Thalassiosira weissflogii* and *T. pseudonana* showed that the boron content of cultured opal was significantly lower than suggested by the bulk sampling of Ishikawa and Nakamura (1993) at around 5-10 ppm, increasing as pH increased from 7.6 to 8.7 (Mejia et al. 2013; Supplementary Figure S1). This suggests seawater tetrahydroxyborate anion (borate; $B(OH)_4^-$) is predominantly incorporated into the diatom frustule rather than boric acid ($B(OH)_3$), and implies there is potential for the boron content of diatom opal to trace pH in the past (Mejia et al. 2013).

Here, the relationship between $\delta^{11}B$ of the frustules of the diatom *T. weissflogii* and seawater pH is investigated for the first time using a batch culturing technique and different air-CO_2 mixtures to explore a range of pH (8.54 ± 0.57 to 7.48 ± 0.06). The aim of this study was also to develop a methodology for measuring the boron isotopic composition of biogenic silica by MC-ICP-MS and apply this method to explore the response of the boron based proxies ([B] and $\delta^{11}B$) in diatom frustules to changing pH. Ultimately, we show how boron isotopes measured in diatom frustules may provide further insight into boron uptake and physiological activity within diatoms, and we test the potential of $\delta^{11}B$ and boron content in diatoms as proxies for the ocean carbonate system.

2. Methods

2.1 Experimental Set up

The centric diatom *T. weissflogii* (Grunow in van Heurck, PCC 541, CCAP 1085/1; Hasle and Fryxell, 1977) was grown in triplicate in K/1 enriched sterile and filtered seawater (0.2 μm; seawater sourced from Labrador Sea; Keller et al., 1987) in 3 L glass Erlenmeyer flasks for a maximum of one week for each experiment. Initial nutrient concentrations within the seawater before enrichment were assessed on a SEAL Analytical QuAAtro analyser with a UV/vis spectrometer and ranged from 23.3 to 27.5 µM for nitrate(+nitrite), 4.3 to 5.4 µM for silicic acid, and 1.4 to 1.6 µM for phosphate. The culture experiments were bubbled with air-CO_2 mixtures in different concentrations (sourced from BOC) to provide a pH range at constant bubble rates, and every flask was agitated by hand twice daily to limit algal settling and aggregation. The monocultures were grown in nutrient replete conditions at

constant temperature (20°C) and on a 12h:12 h light:dark cycle (with 192 μE m^{-2} s^{-1}, or 8.3 E m^{-2} d^{-1} during the photoperiod). The diatoms were acclimated to each pCO_2 treatment for at least 10 generations before inoculating the culture experiment flasks. All culture handling was completed within a laminar flow hood to ensure sterility. The flow hood surfaces were cleaned with 90% ethanol before and after handling, as well as the outer surface of all autoclaved labware entering the laminar flow hood such as bottles and pipettes.

The cultured diatom samples were collected by centrifugation at 96 h, during the exponential phase. Each flask was simultaneously disconnected from the gas supply, and the culture was immediately centrifuged at 3700 rpm for 30 minutes into a pellet, rinsed with MilliQ, and frozen at -20°C in sterile plastic 50 mL centrifuge tubes. Around 10 mg of diatom was harvested in each experiment.

2.2. Growth rate and cell size

A 5 mL sub-sample was taken from each culture flask through sterilised Nalgene tubing into sterile syringes, and sealed in sterile 15 mL centrifuge tubes. Triplicate cell counts using a Coulter Multizier™3 (Beckman Coulter) were performed daily on each experimental flask. Growth rates were calculated using equation 1:

$$\mu = (lnN_t - lnN_i)/(t - t_i) \quad (1)$$

Where N_i is the initial cell density at the start of the experiment (t_i) and N_t is the cell density at time t. Triplicate estimates of cell size were also determined using the Coulter Multizier™3, to determine the mean cell size over time in each flask. Figure 1 shows that although there is no statistically significant relationship between pH and diatom growth rate, cell size does show a small, but statistically significant, positive slope.

2.3 pH, DIC and $\delta^{11}B$ of the culture media

A pH meter (Orion 410A) calibrated using standard National Bureau of Standards (NBS) buffers prior to sample extraction was used to monitor the evolution of pH through the experiment on a daily basis. For fully quantitative constraints on the carbonate system of the culture media, dissolved inorganic carbon; DIC) was measured in triplicate, every other day, for each pH treatment (*i.e.* one per experiment flask). The 100 mL bottles were filled to overflowing and immediately closed with ground glass stoppers, then uncapped to be poisoned with 1 mL mercuric chloride ($HgCl_2$) to prevent any further biologically-induced changes in DIC and stored sealed with Apiezon L grease in complete

darkness until analysis. Analysis of DIC was performed by acidification with excess 10% phosphoric acid and CO_2 transfer in a nitrogen gas stream to an infrared detector using a DIC Analyzer AS-C3 (Apollo SciTech, DE, USA) at the University of Southampton. The DIC results were calibrated using measurements of batch 151 certified reference material obtained from A. G. Dickson (Scripps Institution of Oceanography, CA, USA). The accuracy of the DIC analysis was c. 3 µmol kg^{-1}. Carbonate system parameters, including seawater pCO_2, were calculated using measured pH_{NBS} and DIC values, temperature, salinity and nutrients with the CO_2SYS v1.1 programme (van Heuven et al., 2011; using constants from Dickson, 1990; Lueker et al., 2000; Lee et al., 2010), which was also used to convert pH from the NBS to the Total scale (used throughout).

All flasks were initially filled with media from the same large batch, and all culture treatments therefore started with the same initial pH. The pH for all treatments was then altered by bubbling through the different air-CO_2 mixtures, ranging from low pH (target = 1600 ppm, high pCO_2) to high pH (target = 200 ppm, low pCO_2). Almost all treatments held relatively constant DIC and pH until the final 24 hours of the experiment, when marked changes in DIC and pH in all culture treatments were observed (Figure 2), which in most cases was likely due to the growth of diatoms and an associated net removal of DIC, despite the constant addition of pCO_2. In order to account for these non-steady state conditions of the carbonate system, the mean pH and pCO_2 of each treatment were calculated based on the number of cells grown per 24 hours along with the pH/pCO_2 measured in that 24 hours, thus adjusting for the observed exponential growth rate of *T. weissflogii* (Table 1).

The boron concentration of the culture media was not determined but is assumed to be the same as Labrador seawater (~4.5 ppm; Lee et al. 2010). The boron isotopic composition of the culture media was determined using standard approaches (Foster et al., 2010) to be 38.8 ± 0.19 ‰ (2 s.d.).

2.4 Preparing cultured diatoms for $\delta^{11}B$ and B/Si analysis

In order to examine reproducibility and accuracy of our boron measurements, an in-house diatom reference material was used to develop a method for measuring boron isotopes and boron concentration in biogenic silica. A British Antarctic Survey core catcher sample (TC460) from core TC460 in the Southern Ocean (-60.81534° N, -50.9851° E, water depth 2594 m) was used for this purpose (supplied by C.-D. Hildebrand [British Antarctic Survey]). Although the diatom assemblage was not characterised in the core catcher, the nearest sediment sample in the core is dominated by *Hyalochaete Chaetoceros* resting spores, representing circa 70% of the total diatom content, with sea ice and cool open water species making up the bulk of the remaining 30% (*e.g. Actinocyclus actinochilus, Fragilariopsis curta, F. cylindrus, F. obliquecostata, Odontella weissflogii, Thalassiosira*

166 *antarctica*). A pure diatom sample of mixed species was separated from this bulk sediment and
167 cleaned of clay contamination at the University of Nottingham following an established diatom
168 separation technique (Swann et al., 2013). Briefly, the bulk sample underwent organic removal and
169 carbonate dissolution (using 30% H_2O_2 and 5% HCl), heavy liquid separation in several steps at
170 different specific gravities using sodium polytungstate (SPT), and visual monitoring throughout the
171 process to ensure the sample was free from non-diatom material, such as clay particulates. After the
172 final SPT separation, samples were rinsed thoroughly with MilliQ and sieved at 10 µm to remove all
173 SPT traces.
174
175 The culture samples and the diatom fraction from TC460 were first acidified (H_2SO_4), and organics
176 were oxidised using potassium permanganate and oxalic acid (following Horn et al., 2011 and Mejía
177 et al., 2013). The samples were rinsed thoroughly using MilliQ water via centrifugation and transferred
178 to acid-cleaned Teflon beakers. A secondary oxidation was completed under heat using perchloric
179 acid. Finally, the organic-free samples were rinsed thoroughly with MilliQ via filtration.
180
181 In the boron-free HEPA filtered clean laboratory at the University of Southampton, each sample was
182 dissolved completely in a gravimetrically known amount of NaOH (0.5 M from 10 M concentrated
183 stock supplied by Fluka) at 140°C for 6 to 12 h, and briefly centrifuged prior to boron separation to
184 ensure no insoluble particles were loaded onto the boron column. Anion exchange columns containing
185 Amberlite IRA 743 resin were then used to separate the matrix from the boron fraction of each sample
186 following Foster (2008). Briefly, the dissolved opal was loaded directly onto the column without
187 buffering and the matrix removed with 9 x 200 µL washes of MilliQ. This was collected for subsequent
188 analysis and the pure boron fraction was then eluted and collected in 550 µL of 0.5 M HNO_3 acid. The
189 level of potential contamination was frequently monitored using total procedural blanks (TPB)
190 measured in every batch of columns. The TPB comprised an equivalent volume of sodium hydroxide
191 (NaOH, 0.5 M) as used in the samples of each batch (ca. 0.2 - 4 mL). This was analysed following the
192 sample analysis protocols detailed below, and typically the TPBs for this work contained less than 40
193 pg of boron. This equates to a typical blank contribution of ca. 0.015%, which results in a negligible
194 correction and is therefore ignored here.
195
196 Prior to isotope analysis, all boron fractions were collected in pre-weighed acid cleaned Teflon beakers
197 and their mass was recorded using a Precisa balance. A 10 µL aliquot was taken and diluted with 490
198 µL 0.5 M HNO_3 in acid cleaned plastic centrifuge tubes (2 mL). This was then analysed using a Thermo
199 Fisher Scientific Element 2XR ICP-MS at the University of Southampton, with boron concentration

Biogeosciences Discuss., https://doi.org/10.5194/bg-2019-180
Manuscript under review for journal Biogeosciences
Discussion started: 23 May 2019

200 determined using standard approaches and a gravimetric standard containing boron, silicon, sodium,
201 and aluminium. In order to determine the B/Si ratio, and hence the B concentration of the opal, the
202 Si concentration must also be quantitatively measured. This is achieved here by using a known
203 concentration and mass of NaOH to dissolve each sample, and by measuring the Si/Na ratio the Si
204 concentration of each opal sample can be determined. From this, assuming a chemical formula of
205 $SiO_2.H_2O$ and a H_2O content of 8% (Hendry and Anderson, 2013), the B content of the opal in ppm can
206 be estimated. As detailed above, during the purification procedure, sample matrix was washed off
207 the column using MilliQ, and collected in pre-weighed acid cleaned Teflon beakers. These samples
208 were then diluted with 3 % HNO_3 enriched with Be, In and Re for the internal standardisation and
209 measured on the Thermo Scientific X-series ICP-MS. The standards run on the X-Series consisted of
210 varied concentrations of the gravimetric standard also used on the Element, containing B, Si, Na and
211 Al.
212
213 The boron isotopic composition of the biogenic silica samples was determined on a Thermo Scientific
214 Neptune MC-ICP-MS, also situated in a boron-free HEPA filtered laboratory at the University of
215 Southampton, following Foster (2008). Instrument induced fractionation of the $^{11}B/^{10}B$ ratio was
216 corrected using a sample-standard bracketing routine with NIST SRM 951, following Foster (2008).
217 This allows a direct determination of $\delta^{11}B$ without recourse to an absolute value for NIST SRM 951
218 (Foster, 2008) using the following equation, where $^{11}B/^{10}B_{standard}$ is the mean $^{11}B/^{10}B$ ratio of the
219 standards bracketing the sample of interest.
220
221 $$\delta^{11}B = \left[\left(\frac{^{11}B/^{10}B_{sample}}{^{11}B/^{10}B_{standard}}\right) - 1\right] \times 1000 \quad (2)$$
222
223 The reported $\delta^{11}B$ is an average of the two analyses, with each representing a fully independent
224 measurement (*i.e.* the two measurements did not share blanks or bracketing standards). Machine
225 stability and accuracy was monitored throughout the analytical session using repeats of NIST SRM 951,
226 as well as boric acid reference materials AE120, AE121 and AE122 that gave $\delta^{11}B$ (± 2 s.d.) of -20.19 ±
227 0.20 ‰, 19.60 ± 0.28 ‰, and 39.31 ± 0.28 ‰, that are within error of the gravimetric values from Vogl
228 and Rosner (2012).
229
230 The reproducibility of the $\delta^{11}B$ and [B] measurements were assessed by repeat measurements of
231 TC460 of different total B concentration (11 to 34 ng of B). In order to assess the accuracy of this
232 method, we follow Tipper et al. (2008) and Ni et al. (2010) and use standard addition. To this end,
233 known amounts of NIST SRM 951 standard were mixed with known quantities of TC460. All mixtures

were passed through the entire separation and analytical procedure, including aliquots of pure standard and sample. A sodium acetate - acetic acid buffer was added to all 951 boric acid used prior to mixing, to ensure the pH was sufficiently elevated for the column separation procedure (following Foster, 2008). The amount of biogenic silica matrix added to the columns for each mixture was kept constant, so the volume added to the column was altered for each mixture accordingly. Uncertainty in the $\delta^{11}B$ calculated for each mixture was determined using a Monte Carlo procedure (n = 1000) in R (R Core Team, 2019) propagating uncertainties, at 95% confidence, in known isotopes ratios (± 0.2 ‰), sample concentration (± 6 %), and measured masses (± 0.5 %).

3. Results and Discussion

3.1 Analytical Technique

3.1.1. Purification

The Na, Si and Al concentration of the matrix fraction of several replicates of the diatom fraction of TC460 are shown in Figure 3a-d. Prior to purification, Na and Si concentrations were consistently around 265 and 114 ppm respectively, whereas Al was more variable at 5-25 ppb. The boron content of these matrix samples in all cases was at blank level. The concentration of these elements in the boron fraction is shown in Figure 3e-g, highlighting that the column procedure is sufficient to concentrate boron and remove Na and Si which are both present at sub 5 ppb level (*i.e.* at less than 0.002 % of matrix concentration). The Al is likely present in the diatom frustule (*e.g.* Koning et al. 2007) and is elevated in the boron fraction compared to the matrix fraction (Figure 3). Diatom-bound Al is likely present as the anion $Al(OH)_4^-$, hence its elevation in the boron fraction. Although this is a detectable level of Al, it is unlikely that this level of contamination will influence the mass fractionation of these samples when measured by MC-ICP-MS (Foster, 2008; Guerrot et al. 2010).

3.1.2. Accuracy and Reproducibility

Throughout the duration of this study, a single dissolution of the diatom fraction of TC460 was measured 18 times in separate analyses at various concentrations, in order to assess external reproducibility of this method. Carbonates generally have a reproducibility of ± 0.20 ‰ (2σ) at an analyte concentration of 50 ppb boron using the MC-ICP-MS methods at Southampton (*e.g.* Chalk et al. 2017). The repeated measurements of TC460 gave a reproducibility of ± 0.28 ‰ (2σ) over 18 samples, ranging from 19 ppb to 61 ppb (11 to 34 ng) boron (Figure 4). The similar $\delta^{11}B$ regardless of boron concentration analysed confirms that blank contamination during purification is not significant. Figure 4 shows that there is also no correlation between Al content of the boron fraction and measured $\delta^{11}B$, confirming Al contamination does not influence mass fractionation.

Figure 4 shows the results of the standard addition experiment, and when the uncertainty in the $\delta^{11}B$ of the mixture is considered, it is clear that nearly all the mixtures lie within error of the 1:1 line, indicating that there is a lack of a significant matrix effect when analysing the $\delta^{11}B$ of biogenic silica as described herein. A least squares linear regression of the mixtures has a slope of 1.01 ± 0.07 and an intercept of -0.15 ± 0.29 ‰, implying the approach is accurate to ± 0.29 ‰, which is remarkably similar to the stated reproducibility of TC460 (± 0.28 ‰ at 2σ).

B and Si content were determined separately and combined post-analysis in order to estimate the B/Si ratio for each sample and hence the B concentration. The reproducibility of this method was tested using six repeats of the diatom fraction of TC460. The mean of all six measurements is 2.99 ± 0.64 ppm; (2σ; Figure 4), implying this multi-stage method of determining the B content of diatoms is precise to ± 20 % at 95% confidence.

3.2. Diatom Cultures

3.2.1. Boron content of the frustule of *T. weissflogii*

The boron content of *T. weissflogii* increases as a function of pH from around ~1 ppm to ~4 ppm over a range of average culture pH from 7.5 to 8.6 (Figure 5; Table 2). While this is lower by an order of magnitude than the limited previous studies of boron in sedimentary diatoms (Ishikawa and Nakamura, 1993), it is similar to boron concentration in the bulk diatom fraction of TC460 (Figure 5) and to that observed in previous culturing studies of this diatom species (Figure 5; Meija et al. 2013). In detail, however, our concentrations are around 2-3 times lower than Meija et al. (2013), perhaps due to the different analytical methods used (laser ablation ICP-MS vs. solution here; Figure A1). Despite the scatter between treatments (also seen in Meija et al. 2013; Figure A1), a least squares regression through the treatments is significant at the 95% confidence level ($y = 2.15x - 15.56$, $R^2 = 0.46$, $p = 0.015$; Figure 5). The cause of this scatter between treatments is not known but a likely contributor is the relatively high variability in the carbonate system which was observed in each treatment due to the growth of the diatoms in this batch culture setup (Figure 2).

Boron is an essential nutrient for diatoms (Lewin, 1966) and it is likely that boric acid passively diffuses across the cell wall to ensure the diatom cell has sufficient boron to meet its biological needs. However, if boric acid were the sole source of boron for the diatoms measured here we might expect a decrease in boron content as pH increases and external dissolved boric acid concentration declines (Figure 6).

Several studies note that a number of higher plants have mechanisms for also actively taking up boron, leading to large variations in internal boron concentrations (Pfeffer et al., 2001; Dordas and Brown, 2000; Brown et al., 2002). Indeed, on the basis of a similar dataset to that collected here, Meija et al. (2013) suggested that borate is likely transported across the cell wall of *T. weissflogii* as some function of external borate concentration, which shows a positive relationship with external pH (Figure 6). This hypothesis is developed and discussed further in the next section.

3.2.2. Frustule $\delta^{11}B$ of *T. weissflogii*

The $\delta^{11}B$ of *T. weissflogii* are isotopically light compared to seawater (39.6 ‰; Foster et al., 2010), with an average value across all treatments of -3.95 ‰ (Table 2). Despite the scatter between treatments, similar to the [B] data, Figure 5 shows that there is a clear relationship between the $\delta^{11}B$ of the diatom frustule and pH (R^2 = 0.43, p <0.01), albeit with a negative and relatively shallow slope (y = -2.37x + 15.34).

These results confirm that biogenic silica, free from clay contamination, has a very light boron isotopic composition (Ishikawa and Nakamura, 1993). However, the observed relationship between $\delta^{11}B$ in *T. weissflogii* and pH is radically different to that which is observed in carbonates (Figure 5), implying a distinctive incorporation mechanism for boron into diatom opal. Much work has been carried out in recent years to show that boron is incorporated in carbonates predominantly as the borate ion with minor, if any, isotopic fractionation (*e.g.* see Branson, 2018 for a review). It is similarly thought that the borate ion is incorporated into opal, in an analogous fashion to its incorporation into clays (Ishikawa and Nakamura, 1993; Kolodny and Chaussidon, 2004). However, such a mechanism in isolation would only be able to generate $\delta^{11}B$ in opal of ~13 ‰ (at lowest pH). Given the preponderance of isotopically light diatoms, radiolaria and chert $\delta^{11}B$ in the literature (including this study; Kolodony and Chaussidon, 2004; Ishikawa and Nakamura, 1993), it is therefore likely that there is an additional light isotopic fractionation of boron on its incorporation into opal, although its absolute magnitude is currently unknown (Kolodony and Chaussidon, 2004).

Without knowledge of the isotopic fractionation of boron on incorporation into biogenic silica, the interpretation of our new $\delta^{11}B$ data is therefore challenging. This difficulty is further increased given that the fluid in the silica deposition vesicle (SDV) in diatoms is unlikely to have the boron isotopic composition of external seawater, and is likely at a relatively acidic pH (~5.5; Meija et al. 2013) to promote polymerisation of $Si(OH)_4$. Nonetheless, the broad similarity between the $\delta^{11}B$ of our cultured

336 *T. weissflogii* with the bulk diatom fraction measured here from sample TC460, and the bulk diatom
337 fraction and radiolarian skeleton measured by Ishikawa and Nakamura (1993), suggests a large part
338 of the light isotopic composition of biogenic silica is driven by the isotopic fractionation on
339 incorporation rather than "vital effects" relating to the $\delta^{11}B$ and pH of the SDV in the different species
340 and organisms. That being said, the >3‰ range between different pH treatments in *T. weissflogii* and
341 the >10 ‰ difference between our *Chaetoceros* dominated bulk diatom fraction from TC460 and the
342 cultured *T. weissflogii,* as well as the negative relationship between pH and diatom $\delta^{11}B$ (Figure 5),
343 argues against a simple two-step model involving the incorporation of seawater borate ion and a fixed
344 isotopic fractionation on incorporation.
345
346 The $\delta^{11}B$ of the fluid from which our *T. weissflogii* precipitated their frustules can be calculated if
347 we assume the pH in the SDV of our *T. weissflogii* is 5.5 across all our treatments (Mejia et al.,
348 2013). This suggests that the isotopic composition of this fluid is lighter than seawater, even if we
349 assume an arbitrary -10 ‰ isotopic fractionation on incorporation (Figure 7a). Furthermore, the
350 $\delta^{11}B$ of the SDV fluid is inversely correlated with the $\delta^{11}B$ of either dissolved borate or dissolved
351 boric acid (Figure 7a).

352 As discussed above, Mejia et al. (2013) suggested that there are two sources of boron in a diatom
353 cell: (i) passively diffused and isotopically heavy boric acid; and (ii) actively incorporated
354 isotopically light borate ion (see Figure 6). Assuming that: (a) no additional fractionation occurs
355 during uptake and diffusion; and (b) only the borate ion is incorporated into the frustule, we can
356 calculate the relative contribution of these two sources of boron as a function of external pH
357 (Figure 7b). This treatment shows that the relative concentration of borate derived boron in the
358 SDV fluid increases as external pH increases, though the absolute values here are a function of
359 the magnitude of the isotopic fractionation on incorporation, and so we only have confidence in
360 the trends shown in Figure 7b. Nonetheless, given that dissolved boric acid concentration
361 decreases and dissolved borate increases as pH is increased (Figure 6), this is perhaps not
362 surprising. This finding is also entirely compatible with the trend of increasing boron content of
363 *T. weissflogii* observed as pH increases (Figure 5).

364 Mejía et al. (2013) proposed that the enrichment of borate ion into the SDV of *T. weissflogii* and *T.*
365 *pseudonana* was the result of the active co-transport of borate ion with bicarbonate ion by
366 bicarbonate transporter proteins. Borate is transported because of its similar charge and size to HCO_3^-
367 and the phylogenetic similarity between bicarbonate and borate transporters (Mejía et al., 2013). In

this model, as external borate ion concentration increases, the borate leak into the diatom cell is also increased. An additional factor is the HCO_3^- transport, which may be proportionally up-regulated as external CO_2 content decreases (as external pH increases) in order to provide the diatom cell with sufficient carbon (Mejía et al., 2013). This may therefore offer an additional factor driving an elevation of the borate content of the SDV as pH increases (Mejía et al., 2013). Regardless of the exact mechanism, a SDV fluid that displays a boron isotopic composition as an inverse function of pH is required to explain the observed $\delta^{11}B$ composition of the frustule of *T. weissflogii* measured here. A simple model whereby external borate ion is an increasingly important contributor to the boron in the SDV as pH increases is able to explain the observed dependency of boron content and $\delta^{11}B$ on pH. However, a more complete model of the boron systematics in diatom opal requires a better understanding of the isotopic fractionations on incorporation of boron into biogenic silica, the environmental controls on this fractionation, and partitioning of the boron into biogenic silica.

3.2.3. Boron based pH proxies in diatom opal

The $\delta^{11}B$-pH and B-pH relationships derived here for *T. weissflogii* potentially offer two independent means to reconstruct the past pH of seawater, particularly in those regions key for CO_2 and heat exchange where foraminifera are largely absent (e.g. the high Southern and Northern latitudes). However, the current calibrations (Figure 5) are relatively uncertain and this may preclude their application to some situations. For instance, recasting the $\delta^{11}B$-pH relationship in terms of $\delta^{11}B$ as the dependent variable and using a regression method that accounts for uncertainty in X and Y variables (SIMEX; Carroll et al., 1996) gives the calculated residual pH of the regression as ± 0.28 pH units. For the [B] vs. pH relationship, this uncertainty is ± 0.36 pH units. At TA or DIC typically found in the surface ocean such a variability in pH would translate to estimated seawater pCO_2 of ca. ± 250 ppm. Although encouraging, this treatment suggests that additional work is needed before the relationship between $\delta^{11}B$ and boron content of diatom opal and seawater pH is a sufficiently precise proxy for a fully quantitative past ocean pH. In particular, future culturing efforts should aim to more carefully control the pH of the culture media. This could be achieved by either using larger volume dilute batch cultures, and/or by harvesting the diatoms earlier in the experiment prior to any significant drift in the carbonate system, or more robustly through using a steady state chemostat method (Leonardos and Geider, 2005).

4. Conclusions

In the first study of its kind, using a modified version of the carbonate boron purification technique of Foster (2008), we show that the $\delta^{11}B$ of *T. weissflogii* opal is pH sensitive but isotopically light (-3.95

‰ on average), and has an inverse relationship with external seawater pH. Using a novel ICP-MS method we also show that the boron content of *T. weissflogii* opal increased with increasing pH, supporting the only other study investigating boron in diatoms (Mejía et al., 2013). This suggests that borate is incorporated into the diatom frustule as the dissolved borate abundance increases with external pH. A simple model is presented, based on Mejía et al. (2013), which implies both of these findings could be due to the boron in the SDV having two distinct sources: external boric acid and external borate ion, with the balance of each source changing with external pH. While these results are encouraging and suggest that the boron proxies in diatom opal may hold considerable promise as a tracer of past ocean pH, more work is needed to fully understand the boron systematics of diatom opal. In particular, there is an urgent need to place boron in opal on a firmer grounding with precipitation experiments in the laboratory at controlled pH to determine the magnitude of boron isotopic fractionation on boron incorporation into opal, and subsequently the dependence of this fractionation on other environmental factors.

Acknowledgements

We wish to thank Claus-Dieter Hildebrand for suppling the diatom rich sediment sample TC460. John Gittins, Mark Stinchcombe, Chris Daniels and Lucie Munns are acknowledged for their help during the culturing and subsequent nutrient and carbonate system analysis. Heather Stoll is also thanked for her useful discussions on this topic. Financial support for this study was provided by the Natural Environmental Research Council (UK) to H.K.D. (grant number 1362080) and to G.L.F. (NE/J021075/1).

Figure Captions

Figure 1. Diatom growth rate and cell size as a function of pH labelled according to CO_2 treatment. Linear least squares regressions, including R^2 and p-values are also shown.

Figure 2: Each culture treatment labelled according to target pCO_2 and showing the evolution in the culture media through the experiment. All treatments exhibit changes in DIC due to diatom growth balanced with the input of pCO_2. The higher pCO_2, the more DIC increases towards the end of the experiment.

Figure 3: (a-d) Concentration of Na, Si, Al and B in the Matrix Fraction by ICP-MS. These analyses suggest blank levels of B are present in the matrix washed off the Amberlite IRA 743 resin-based column. (e-f) Concentration of the Na, Si and Al in the boron fraction indicating blank levels of Na (ca. 1.7 ppb) and Si (ca. 1.9 ppb), and a higher concentration of Al (ca. 68 ppb) are present.

Figure 4: (A) The reproducibility of the TC460 diatom core catcher in-house standard. This shows all samples lie within error of the mean (5.98 ‰ ± 0.28 ‰, 2σ) at varied concentrations. This compares well to carbonates (2σ = 0.20 ‰). (B) Aluminium concentration of the B fraction from TC460 (as ppb of the solution analysed for $\delta^{11}B$) shows no correlation with $\delta^{11}B$, likely suggesting there is no significant effect on mass fractionation for this level of Al. (C) The results of the standard addition experiment. The blue line is a least squares regression between the measured $\delta^{11}B$ of each mixture (green circles) and the calculated $\delta^{11}B$ of that mixture given known end-member values (end members shown as blue circles). $R^2 = 0.97$, $p < 0.0001$, slope = 1.01 ± 0.07 and intercept = -0.15 ± 0.29. 1:1 line is shown as a black line and dotted blue lines show the 95% confidence limit of the regression. Note that the end members were not used in the regression. (D) B content in ppm of six repeat samples of the diatom fraction of TC460. The black line indicates the mean value, and the grey lines show 2σ, of 2.99 ± 0.64 ppm.

Figure 5: (A) $\delta^{11}B$ of *T. weissflogii* diatom opal plotted against aqueous borate, labelled according to pCO_2 treatment. Also shown are published deep sea coral *Desmophyllum dianthus* (Anagnostou et al., 2012) and foraminifera $\delta^{11}B$ (*Globigerinoides ruber* and *Orbulina universa*; Henehan et al., 2013; Henehan et al., 2016, respectively). Least squares regression lines are also shown. (B) Boron content of cultured *T. weissflogii* diatom opal as a function of pH labelled according to pCO_2. A least squares regression with 95% confidence interval is also shown. (C) *T. weissflogii* opal $\delta^{11}B$ against pH of each treatment demonstrating a statistically significant negative relationship. Uncertainty in all points is shown at the 95% confidence level. In some cases, the error bars are smaller than the symbols.

Figure 6: Plots describing (A) the pH-dependent relationship between the abundance of aqueous boron species, and (B) the isotopic fractionation observed between boric acid ($B(OH)_3$; red) and borate ($B(OH)_4^-$; blue) at T = 25 °C and S = 35.

Biogeosciences Discuss., https://doi.org/10.5194/bg-2019-180
Manuscript under review for journal Biogeosciences
Discussion started: 23 May 2019

465 **Figure 7**: (A) Back-calculated $\delta^{11}B$ of the silica deposition vesicle (SDV), and (B) the fraction of boron
466 in the SDV that is derived from external borate. In (A) the diatom $\delta^{11}B$ data are shown as grey circles
467 and the calculated $\delta^{11}B$ of the SDV as blue circles. Included in this model is an arbitrary -10 ‰
468 fractionation between the $\delta^{11}B$ of the SDV and the opal precipitated. The fraction of borate in the
469 SDV in (B) is a function of this assumption so these absolute values should be taken as illustrative
470 only.
471
472
473

Biogeosciences Discuss., https://doi.org/10.5194/bg-2019-180
Manuscript under review for journal Biogeosciences
Discussion started: 23 May 2019

474 **Tables**

475

Treatment	pCO_2 (ppm)	2σ	pH	2σ	DIC (μM)	2σ	HCO_3^- (μM)	2σ	Growth rate (d^{-1})
200	125	8	8.53	0.73	1925	61	1091	59	1.03
280	244	73	8.25	0.41	2165	113	1521	260	1.03
400	267	28	8.25	0.44	2400	115	1728	107	0.96
800	809	62	7.83	0.24	2525	56	2206	69	1.01
1600	2117	40	7.48	0.08	2791	21	2628	22	1.01

476 *Table 1: Mean carbonate system parameters experienced under the average growth*
477 *conditions as calculated for each culture treatment on the basis of the number of cells*
478 *grown in each 24-hour period of the batch experiment.*

479

Treatment	pH (Total scale)	pH 2σ	$\delta^{11}B$	$\delta^{11}B$ 2σ	$\delta^{11}B$ sw borate	[B] ppm
200	8.55	0.63	-5.51	0.21	24.20	3.15
200	8.54	0.62	-5.40	0.21	24.00	2.81
280	8.27	0.35	-5.05	0.20	20.00	3.72
280	8.18	0.25	-5.66	0.21	18.80	0.93
280	8.30	0.42	-5.79	0.21	20.50	1.04
400	8.26	0.38	-3.64	0.20	19.90	3.37
400	8.24	0.36	-3.57	0.21	19.60	1.26
400	8.25	0.36	-2.41	0.21	19.70	2.68
800	7.85	0.22	-2.93	0.19	15.40	NA
800	7.82	0.18	-2.80	0.22	15.20	0.78
800	7.82	0.20	-3.08	0.21	15.20	1.11
1600	7.48	0.06	-1.94	0.20	13.30	0.74
1600	7.48	0.07	-3.62	0.21	13.30	0.91

480 *Table 2. Treatment name and pH with $\delta^{11}B$ and [B] for cultured T. weissflogii.*

481

482

483

484

485

References

Anagnostou, E., Huang, K.-F., You, C.-F., Sikes, E. L., and Sherrell, R. M.: Evaluation of boron isotope ratio as a pH proxy in teh deep sea coral Desmophyllum dianthus: Evidence of physiological pH adjustment, Earth Planet. Sci. Lett., 349-350, 251-260, 10.1016/j.epsl.2012.07.006, 2012.

Bradshaw, A. L., Brewer, P. G., Schafer, D. K., and Williams, R. T.: Measurements of total carbon dioxide and alkalinity by potentiometric titration in the GEOSECS program, Earth Planet. Sci. Lett., 55, 99-115, 1981.

Branson, O.: Boron Incorporation into Marine CaCO3, in: Boron Isotopes: The Fifth Element, edited by: Marschall, H., and Foster, G., Springer International Publishing, Cham, 71-105, 2018.

Brown, P. H., Bellaloui, N., Wimmer, M. A., Bassil, E. S., Ruiz, J., Hu, H., Pfeffer, H., Dannel, F., and Romheld, V.: Boron in plant biology, Plant Biology, 4, 205-223, 2002.

Carroll, R. L., Kuchenhoff, H., Lombard, F., and Stefanski, L. A.: Asymptotics for the SIMEX Estimator in Nonlinear Measurement Error Models, Journal of the American Statistical Association, 91, 242-250, 1996.

Chalk, T. B., Hain, M. P., Foster, G. L., Rohling, E. J., Sexton, P. F., Badger, M. P. S., Cherry, S. G., Hasenfratz, A. P., Haug, G. H., Jaccard, S. L., Martínez-García, A., Pälike, H., Pancost, R. D., and Wilson, P. A.: Causes of ice age intensification across the Mid-Pleistocene Transition, Proceedings of the National Academy of Sciences, 10.1073/pnas.1702143114, 2017.

Dickson, A. G.: Thermodynamics of the dissociation of boric acid in synthetic seawater from 273.15 to 318.15 K, Deep Sea Research Part A. Oceanographic Research Papers, 37, 755-766, 1990.

Dordas, C., and Brown, P. H.: Permeability of boric acid across lipid bilayers and factors affecting it, J. Membr. Biol., 175, 95-105, 2000.

Foster, G. L.: Seawater pH, pCO2 and [CO32-] variations in the Caribbean Sea over the last 130 kyr: A boron isotope and B/Ca study of planktic foraminifera, Earth Planet. Sci. Lett., 271, 254-266, 2008.

Foster, G. L., Pogge von Strandmann, P. A. E., and Rae, J. W. B.: Boron and magnesium isotopic composition of seawater, Geochemistry Geophysics Geosystems, 11, Q08015, doi:08010.01029/02010GC003201, 2010.

Gray, W. R., Rae, J. W. B., Wills, R. C. J., Shevenell, A. E., Taylor, B., Burke, A., Foster, G. L., and Lear, C. H.: Deglacial upwelling, productivity and CO2 outgassing in the North Pacific Ocean, Nature Geoscience, 11, 340-344, 10.1038/s41561-018-0108-6, 2018.

Guerrot, C., Milot, R., Robert, M., and Negrel, P.: Accurate and high-precision determination of boron isotopic ratios at low concentration by MC-ICP-MS (Neptune), Geostandards and Geoanlaytical Research, 35, 275-284, 2010.

Hasle, G. R., and Fryxell, G. A.: The genus Thalassiosira: some species with a linear areola array, Proceedings of the Fourth Symposium on Recent and Fossil Marine Diatoms, Oslo, 1977, 15-66,

Hemming, N. G., and Hanson, G. N.: Boron isotopic composition and concentration in modern marine carbonates, Geochimica et Cosmochimica Acta, 56, 537-543, 1992.

Hendry, K. R., and Andersen, M. B.: The zinc isotopic composition of siliceous marine sponges: Investigating nature's sediment traps, Chem. Geol., 354, 33-41, 2013.

Henehan, M. J., Rae, J. W. B., Foster, G. L., Erez, J., Prentice, K. C., Kurcera, M., Bostock, H. C., Martinez-Boti, M. A., Milton, J. A., Wilson, P. A., Marshall, B., and Elliott, T.: Calibration of the boron isotope proxy in the planktonic foraminifera Globigerinoides ruber for use in palaeo-CO2 reconstruction, Earth Planet. Sci. Lett., 364, 111-122, 10.1016/j.epsl.2012.12.029, 2013.

Henehan, M. J., Foster, G. L., Bostock, H. C., Greenop, R., Marshall, B., and Wilson, P. A.: A new boron isotope-pH calibration for Orbulina universa, with implications for understanding and accounting for vital effects, Earth Planet. Sci. Lett., 454, 282-292, 10.1016/j.epsl.2016.09.024, 2016.

Honisch, B., and Hemming, N. G.: Surface ocean pH response to variations in pCO2 through two full glacial cycles, Earth Planet. Sci. Lett., 236, 305-314, 2005.

Horn, M. G., Robinson, R. S., Rynearson, T., and Sigman, D. M.: Nitrogen isotopic relationship between diatom-bound and bulk organic matter of cultured polar diatoms, Paleoceanography, 26, 1-12, 2011.

Ishikawa, T., and Nakamura, E.: Boron isotope systematics of marine sediments, Earth Planet. Sci. Lett., 117, 567-580, 1993.

Keller, M. D., Selvin, R. C., Claus, W., and Guillard, R. R. L.: Media for the culture of oceanic ultraplankton, Journal of Phycology, 23, 633-638, 1987.

Kolodny, Y., and Chaussidon, M.: Boron isotopes in DSDP cherts: Fractionation and diagenesis, The Geochemical Society Special Publications, 9, 1-14, 2004.

Koning, E., Gehlen, M., Flank, A.-M., Calas, G., and Epping, E.: Rapid post-mortem incorporation of aluminium in diatom frustules: evidence from chemical and strutural analyses, Mar. Chem., 106, 208-222, 10.1016/j.marchem.2006.06.009, 2007.

Lee, K., Kim, T.-W., Byrne, R. H., Millero, F. J., Feely, R. A., and Liu, Y.-M.: The universal ratio of boron to chlorinity for the North Pacific and North Atlantic oceans, Geochimica et Cosmochimica Acta, 74, 1801-1811, 2010.

Leonardos, N., and Geider, R. J.: Elevated atmospheric carbon dioxide increases organic carbon fixation by Emiliania huxleyi (haptophyta), under nutrient-limited high-light conditions, Journal of Phycology, 41, 1196-1203, 10.1111/j.1529-8817.2005.00152.x, 2005.

Lewin, J.: Boron as a growth requirement for diatoms, Journal of Phycology, 2, 160-163, 10.1111/j.1529-8817.1966.tb04616.x, 1966.

Lueker, T. J., Dickson, A. G., and Keeling, C. D.: Ocean pCO2 calculated from dissolved inorganic carbon, alkalinity, and equations for K1 and K2: validation based on laboratory measurements of CO2 gas and seawater at equilibrium Mar. Chem., 70, 105-119, 2000.

Martin, J.: Glacial-interglacial CO2 change: The iron hypothesis, Paleoceanography, 5, 1-13, 1990.

Martinez-Boti, M. A., Marino, G., Foster, G. L., Ziveri, P., Henehan, M. J., Rae, J. W. B., Mortyn, P. G., and Vance, D.: Boron isotope evidence for oceanic carbon dioxide leakage during the last deglaciation, Nature, 518, 219-222, 10.1038/nature14155, 2015.

Mejia, L. M., Isensee, K., Menendez-Vicente, A., Pisonero, J., Shimizu, N., Gonzalez, C., Monteleone, B. D., and Stoll, H.: B content and Si/C ratios from cultured diatoms (Thalassiosira pseudonana and Thalassiosira weissflogii): Relationship to seawater pH and diatom carbon acquisition, Geochmica et Cosmochimca Acta, 123, 322-337, 10.1016/j.gca.2013.06.011, 2013.

Ni, Y., Foster, G. L., and Elliott, T.: The accuraccy of d11B measurements of foraminifers, Chem. Geol., 274, 187-195, 2010.

Pearson, P. N., and Palmer, M. R.: Atmospheric carbon dioxide concentrations over the past 60 million years, Nature, 406, 695 - 699, 2000.

Pfeffer, H., Daniel, F., and Romheld, V.: Boron compartmentation in roots of sunflower plants of different boron status: A study using the stable isotopes 10B and 11B adopting two independent approaches Physiol. Plant., 113, 346-351, 2001.

Rae, J. W. B., Foster, G. L., Schmidt, D. N., and Elliott, T.: Boron isotopes and B/Ca in benthic foraminifera: proxies for the deep ocean carbonate system, Earth Planet. Sci. Lett., 302, 403-413, 2011..

R Core Team (2018). R: A language and environment for statistical computing. R Foundation for Statistical Computing, Vienna, Austria. URL https://www.R-project.org/.

576 Sigman, D. M., and Boyle, E. A.: Glacial/Interglacial variations in atmospheric carbon dioxide, Nature,
577 407, 859-869, 2000.

578 Sigman, D. M., Hain, M. P., and Haug, G. H.: The polar ocean and glacial cycles in atmospheric CO2
579 concentration, Nature, 466, 47-55, doi:10.1038/nature09149, 2010.

580 Sosdian, S. M., Greenop, R., Hain, M. P., Foster, G. L., Pearson, P. N., and Lear, C. H.: Constraining the
581 evolution of Neogene ocean carbonate chemistry using the boron isotope pH proxy, Earth Planet. Sci.
582 Lett., 248, 362-376, doi:10.1016/j.epsl.2018.06.017, 2018.

583 Swann, G. E. A., Pike, J., Snelling, A. M., Leng, M. J., and Williams, M. C.: Seasonally resolved diatom
584 d18O records from the West Antarctic Peninsula over the last deglaciation, Earth Planet. Sci. Lett.,
585 364, 12-23, 10.1016/j.epsl.2012.12.016, 2013.

586 Tipper, E. T., Galy, A., and Bickle, M.: Calcium and magnesium isotope systematics in rivers draining
587 the Himalaya-Tibetan-Plateau region: Lithological or fractionation control?, Geochmica et
588 Cosmochimca Acta, 72, 1057-1075, 2008.

589 van Heuven, S., Pierrot, D., Rae, J. W. B., Lewis, E., and Wallace, D. W. R.: MATLAB Program Developed
590 for CO2 System Calculations, 10.3334/CDIAC/otg.CO2SYS_MATLAB_v1.1, 2011.

591 Vogl, J., and Rosner, M.: Production and certificaiton of a unique set of isotope and delta reference
592 materials for boron isotope determination in geochemical, environmental and industrial materials,
593 Geostandards and Geoanlaytical Research, 36, 161-175, 2012.

594

Biogeosciences Discuss., https://doi.org/10.5194/bg-2019-180
Manuscript under review for journal Biogeosciences
Discussion started: 23 May 2019

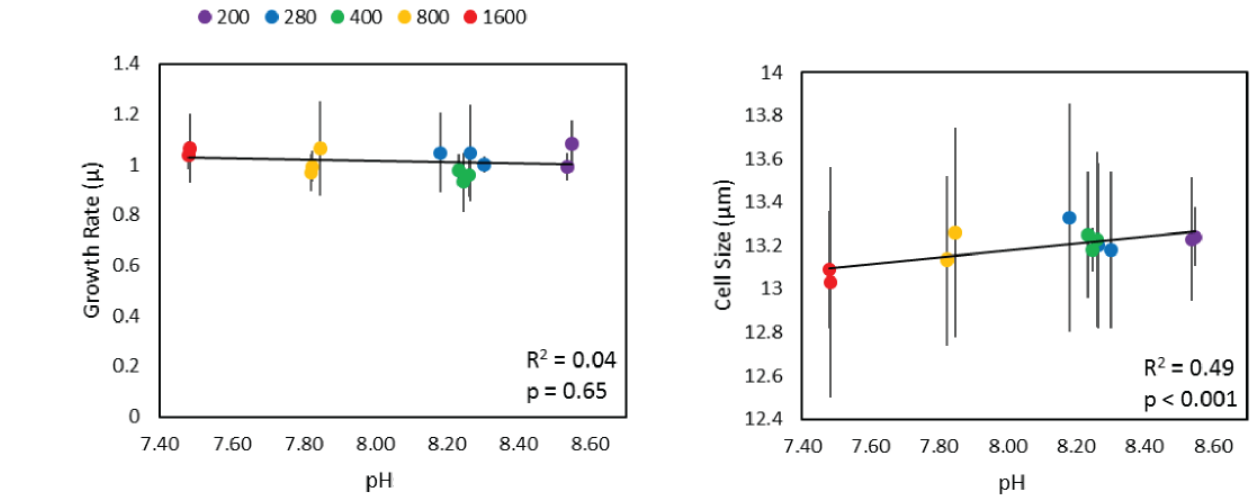

Figure 1

Biogeosciences Discuss., https://doi.org/10.5194/bg-2019-180
Manuscript under review for journal Biogeosciences
Discussion started: 23 May 2019

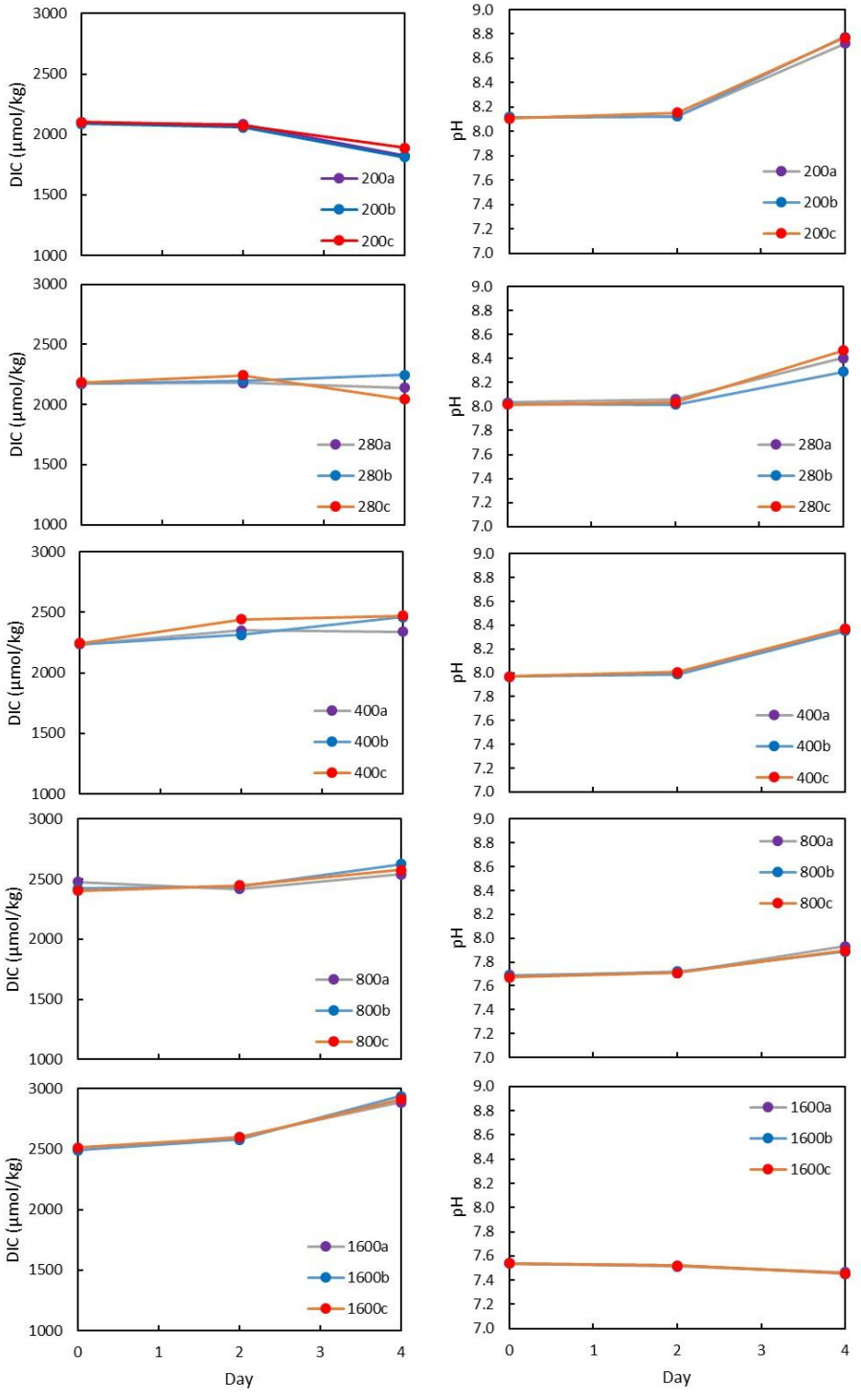

Figure 2

Biogeosciences Discuss., https://doi.org/10.5194/bg-2019-180
Manuscript under review for journal Biogeosciences
Discussion started: 23 May 2019

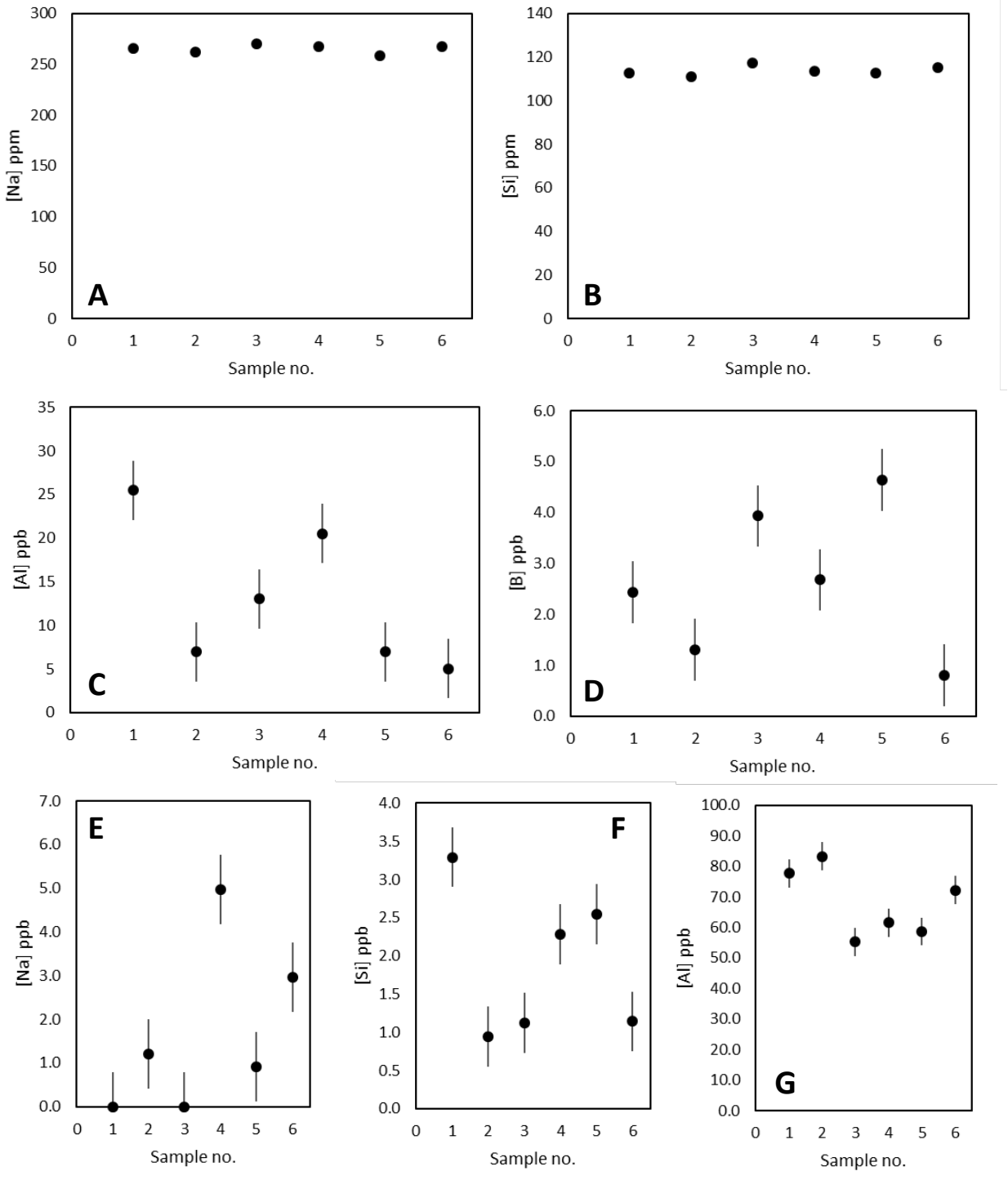

Figure 3.

Biogeosciences Discuss., https://doi.org/10.5194/bg-2019-180
Manuscript under review for journal Biogeosciences
Discussion started: 23 May 2019

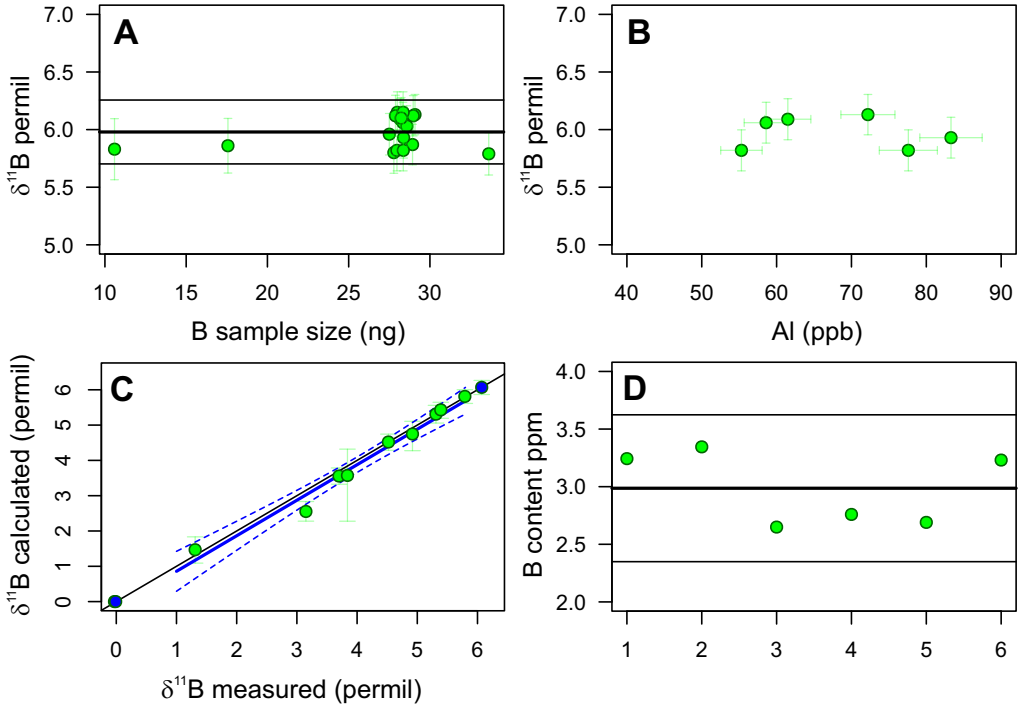

Figure 4

Biogeosciences Discuss., https://doi.org/10.5194/bg-2019-180
Manuscript under review for journal Biogeosciences
Discussion started: 23 May 2019

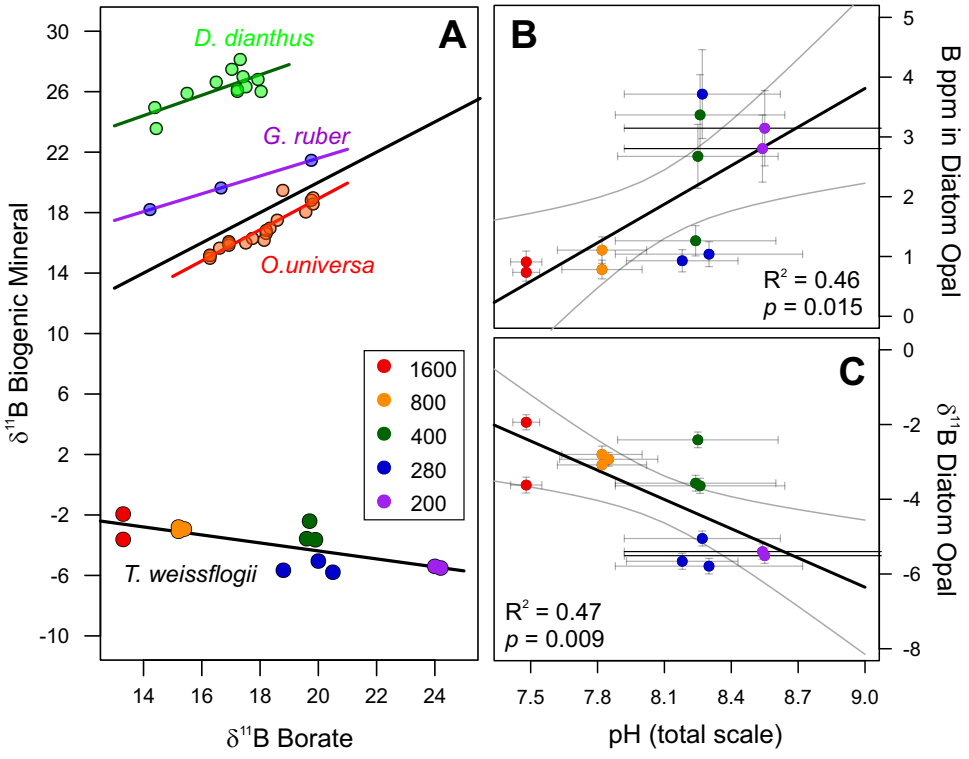

Figure 5.

Biogeosciences Discuss., https://doi.org/10.5194/bg-2019-180
Manuscript under review for journal Biogeosciences
Discussion started: 23 May 2019

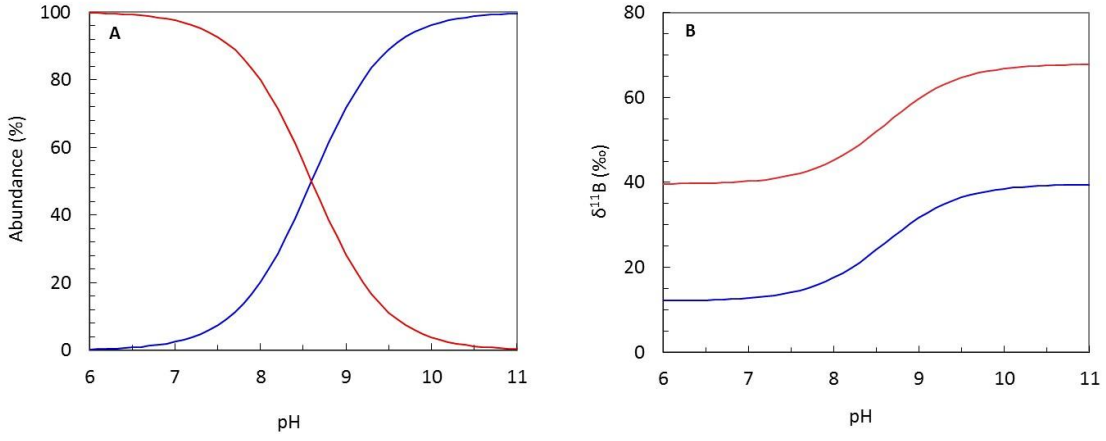

Figure 6.

Biogeosciences Discuss., https://doi.org/10.5194/bg-2019-180
Manuscript under review for journal Biogeosciences
Discussion started: 23 May 2019

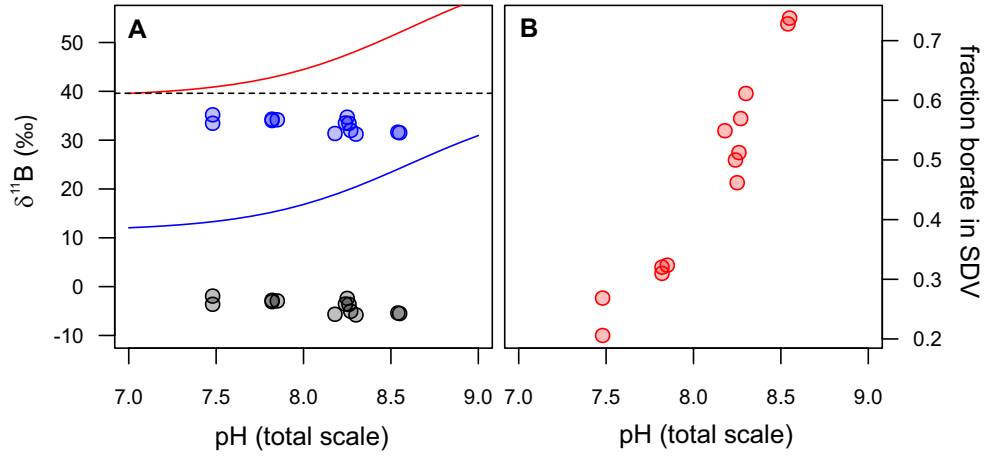

Figure 7.